*Biochimica et Biophysica Acta*, 1023 (1990) 421–435
Elsevier



BBAMEM 74791

# Injury-induced vesiculation and membrane redistribution in squid giant axon

Harvey M. Fishman, Kirti P. Tewari and Philip G. Stein

*Department of Physiology and Biophysics, University of Texas Medical Branch, Galveston, TX (U.S.A.)*

(Received 5 June 1989)
(Revised manuscript received 11 October 1989)

Key words: Axosome; Vesiculation; Fusion; Ion channel; Membrane redistribution; Neural injury; Differential interference contrast; (Squid axon)

**Injury of isolated squid giant axons in sea water by cutting or stretching initiates the following unreported processes: (i) vesiculation in the subaxolemmal region extending along the axon several mm from the site of injury, followed by (ii) vesicular fusions that result in the formation of large vesicles (20–50 $\mu$m diameter), 'axosomes', and finally (iii) axosomal migration to and accumulation at the injury site. Some axosomes emerge from a cut end, attaining sizes up to 250 $\mu$m in diameter. Axosomes did not form after axonal injury unless divalent cations ($Ca^{2+}$ or $Mg^{2+}$) were present (10 mM) in the external solution. The requirement for $Ca^{2+}$ and the action of other ions are similar to that for cut-end cytoskeletal constriction in transected squid axons (Gallant, P.E. (1988) J. Neurosci. 8, 1479–1484) and for electrical sealing in transected axons of the cockroach (Yawo, H. and Kuno, M. (1985) J. Neurosci. 5, 1626–1632). Axosomes probably consist of membrane from different sources (e.g., axolemma, organelles and Schwann cells); however, localization of axosomal formation to the inner region of the axolemma and the formation dependence on divalent cations suggest principal involvement of cisternae of endoplasmic reticulum. Patch clamp of excised patches from axosomes liberated spontaneously from cut ends of transected axons showed a 12-pS $K^+$ channel and gave indications of other channel types. Injury-induced vesiculation and membrane redistribution seem to be fundamental processes in the short-term (minutes to hours) that precede axonal degeneration or repair and regeneration. Axosomal formation provides a membrane preparation for the study of ion channels and other membrane processes from inaccessible organelles.**

## Introduction

Cellular mechanisms responsible for degeneration or repair of a previously functional nerve fiber after mechanical damage or pathological disorders are not understood. While a substantial literature exists on long-term (days) processes following axotomy or nerve damage [1], relatively little is known about short-term (minutes to hours) events following nerve damage. The earliest (minutes) known response of a transected unmyelinated nerve fiber is constriction of the cytoskeleton at a cut end [2] and formation of a seal at the site of injury [3]. Seal formation prevents internal accumulation of external ions that are detrimental to membrane excitability [4,5], prevents dissipation of ionic gradients and limits loss of axoplasm and cytoskeletal structures [2]. In transected myelinated fibers the earliest ultrastructural changes associated with degenerating fibers become evident 24 h or more after transection. These ultrastructural changes implicate the Schwann cell as the predominant instrument of axon and myelin destruction [6]. Furthermore, organelles accumulate after two hours on both sides of lesions produced by crushing the sciatic nerve of rats [7]. This accumulation is interpreted as a sign of local reaction, initial degeneration or regeneration or a consequence of migration from distal regions of axons.

In this article we describe additional, early fundamental events, namely vesiculation and membrane redistribution, that accompany cytoskeletal constriction in the cut ends of transected giant axons of cephalopods. In response to axonal injury, membranous vesicles form at the inner region of the axolemma, become larger by fusing, and migrate to the site of injury where they accumulate and occlude the injured region. This process of redistribution involves mobilization of mem-

Correspondence: H.M. Fishman, Department of Physiology, University of Texas Medical Branch, Galveston, TX 77550-2779, U.S.A.

brane from sources in the vicinity of the inner part of the axolemma. Injury-induced vesiculation is significantly reduced in divalent-cation-free media, but addition of $Ca^{2+}$ or $Mg^{2+}$ at extracellular physiological concentrations (10 mM) causes massive vesiculation, vesicular fusions and the formation of large vesicles (20–50 $\mu$m diameter), designated 'axosomes', in injured axons. Based on these observations, we suggest that these processes, newly observed in squid giant axons, may be involved either in axonal degeneration or repair.

Twenty to thirty minutes after transection in artificial sea water (containing divalent cations) some of the accumulated axosomes at cut ends fuse and emerge as giant membranous balls (approx. 100 $\mu$m diameter). Application of a patch-clamp technique [8] to excised patches from axosomes showed currents fluctuating between two discrete levels over a range of membrane voltages with unit conductance (12 pS), reversal potential and affectation by $Zn^{2+}$ that are indicative of a single $K^+$ channel. Discrete-level waveforms from other channel types were also observed in most patches under different ionic conditions, demonstrating that the redistributed membrane contains ion channels, which could play a role in regenerative processes at sites of injury if axosomes were incorporated into a seal. A possible application of harvested axosomes to neurophysiological research may be to provide a membrane preparation for the study of ion channels and other processes from inaccessible membrane sources.

Preliminary reports of this work have been presented [9–12].

## Methods

*Preparations*

Lengths (1.5 to 3 cm) of giant axon originating in the stellate ganglion were dissected, with ends tied, from squid (*Loligo pealei, Loliguncula brevis* and *Sepioteuthis lessoniana*) and cuttlefish (*Sepia officinalis*) as described previously [13]. After fine dissection to remove connective tissue and enhance visibility, axons were placed in a shallow glass dish containing artificial sea water (ASW) for observation in an inverting microscope under phase contrast to assure that vesiculation had not been initiated as a result of injury during dissection. Unvesiculated axons were transferred to another dish containing test solution and stressed in one of two ways: (1) by stretching to twice the resting length by holding each tied end with separate forceps while moving both hands simultaneously and rectilinearly in opposite directions so that the motion of each hand in time was sinusoidal for 3–5 cycles or (2) by cutting with scissors into 3 to 5 mm segments. Observations of axon segments were made with the segments in a solution-filled 35 mm-diameter shallow, glass dish with cover slip (to prevent evaporation) using either phase contrast (Olympus CK2) or differential-interference-contrast (DIC) (Zeiss 405M Axiovert) microscopy. Photomicrographs were obtained by conventional photography and by photographing single 'freezed frames' from video tape recordings (JVC HR-D440U) which were displayed on a video monitor.

*Solutions*

The standard bath solution, artificial sea water (ASW), was composed of the following (in mM): 430 NaCl, 10 KCl, 10 $CaCl_2$, 50 $MgCl_2$, and 5 TrisCl buffered to pH 7.4 at 22° C. A K-ASW consisting of: 440 KCl, 10 $CaCl_2$, 50 $MgCl_2$, and 5 TrisCl was used in patch clamp pipets. Glutamate salts of univalent ions were used to replace $Cl^-$, calcium gluconate was substituted for $CaCl_2$ and $MgSO_4$ replaced $MgCl_2$. Both solutions contained 1 $\mu$M tetrodotoxin (TTX) to eliminate conduction in voltage-sensitive $Na^+$ channels. Because of their well established behavior in suppressing $K^+$ conduction in the squid axon axolemma, tetraethylammonium (TEA) and 3,4-diaminopyridine (DAP) were added separately to bath and patch pipet solutions in order to aid in the identification of $K^+$ channels in excised patches from axosomes. Addition of $Zn^{2+}$ to the bath was used to induce altered kinetics in $K^+$ channels [14,15]. Bath temperature was measured (20–26° C) but not controlled.

*Patch voltage clamp [8] of axosomes*

Micropipets were drawn from Corning type 7052 glass capillaries and the tips were fire polished to a few tenths of a $\mu$m in diameter. Axosomes emerged spontaneously from the cut end of axons 20–30 min after transection in ASW, and formed stable attachments to the cut end via cytoskeletal debris. Electrical isolations ('seals') of axosomal patches, in regions free of cytoskeletal debris, of about 100 gigohms were common and often stable for several hours. Patches with seals of less than 30 gigohms were not used. After seal formation patches were excised from axosomes in an inside-out configuration by withdrawal of the pipet tip from the axosomal surface. The bath was driven by a voltage source through a Ag-AgCl pellet in 3 M KCl solution connected to the bath by an agar-salt bridge. Current from electrically isolated patches of the external surface of axosomes, was recorded by a discrete-component, low-noise operational amplifier (op amp) of our own design, in the transresistance mode with a 3 gigohm resistor (National Micronetics) as the feedback element. The uncompensated bandwidth (−3 dB) of the transresistance op amp was determined to be 450 Hz by injection of a synchronized, synthesized signal [16] through an air capacitor into the inverting input of the op amp and by determining the frequency at which the phase angle of the output deviated by 45° from an ideal capacitive response. The op amp was followed by a gain (10 ×) stage. Frequency compensation of the transresis-

tance op amp response was not used because the channel events reported here were within the uncompensated bandwidth and because no compensation was preferable to the distortion that can arise from compensation schemes. The uncompensated output of the gain stage was stored by a frequency-modulated (FM) tape recorder (HP3960) (cutoff at 1.25 kHz). Single-channel analog recordings from FM tape were digitized using a Metrabyte (model DASH-16) analog-to-digital converter board within the backplane of an IBM AT computer and under control of Metrabyte program 'STREAMER'. The analog records were sampled at 3.0 kHz for about 20 s, yielding digitized files of 128 kbytes (2 bytes/sample). Digitized files calibrated as current flow (in pA) through the patch pipet were analyzed by use of software in which the crossing of half amplitude of transitions between current levels was the criterion for determination of whether transitions between states (conducting and nonconducting) had occurred. Amplitude histograms of the sampled, patch-current waveforms were produced from entire, unaltered, 128 kbyte digitized files by sorting the current amplitudes into bins and displaying the number of occurrences of a particular amplitude versus bin number.

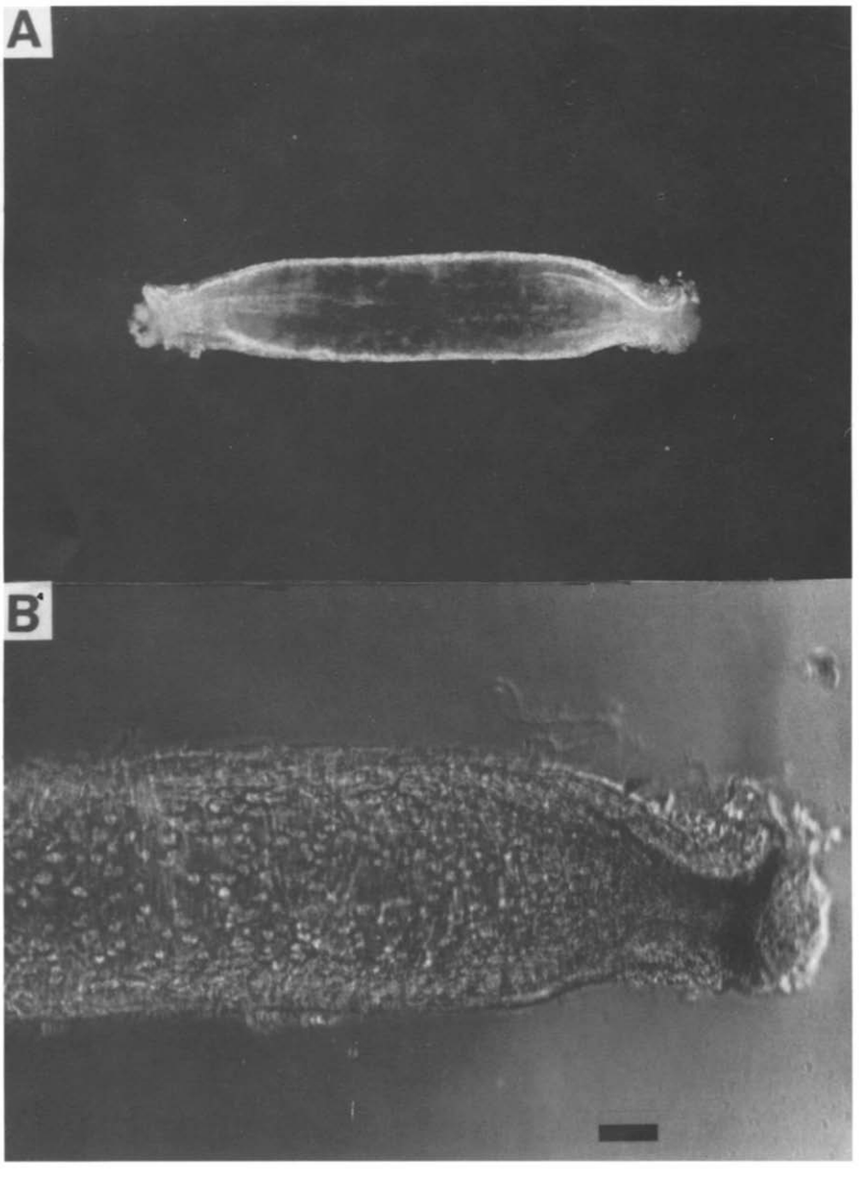


Fig. 1. A 3-mm length axon-segment, cut out of a larger length of squid (*Loligo pealei*) axon in ASW 30 min earlier, as observed (A) by dark-field microscopy and (B) by phase-contrast microscopy. (A) Notice constricted ends [2] that scatter more light than the rest of the axon segment but no apparent vesiculation. (B) Phase-contrast micrograph of the same axon segment at a slightly higher magnification and at a focal plane near an inner surface of the axolemma. Vesicles are seen throughout the axon segment. Scale in (B) is 100 $\mu$m and applies only to (B).

## Results

*Injury-induced vesiculation in squid giant axon*

For over fifty years electrophysiologist have inadvertently injured squid giant axons during dissection procedures or during insertion of electrodes. Yet the processes following injury have either been ignored or not observed with the appropriate microscopy. For example, Fig. 1A shows a 3-mm segment of squid giant axon that was cut out of a longer length (3 cm) of isolated (tied-off ends) axon, as viewed through a dark-field light microscope, 30 min after the segment was placed in ASW. As previously reported [2], the ends are noticeably constricted and scatter more light (white appearance) than the unconstricted portion of the axon segment. However, when the same axon segment is examined under phase contrast microscopy with slightly higher magnification and at a focal plane near an inner axolemmal surface (Fig. 1B), vesicles are seen within the entire axon segment (more than half of which is shown in Fig. 1B). Thus, vesiculation occurs within axons transected in ASW, but vesicles are most easily observed via contrast enhanced microscopy. Vesiculation was also apparent after the following types of injuries: (i) cut collaterals, with vesiculation occurring in the vicinity of branch sites in otherwise unvesiculated axons, (ii) mechanically stressed axons by stretching (see Methods), and (iii) partially cut axons, with vesiculation surrounding the resulting small hole (50 $\mu$m diameter) produced with microscissors.

The time development of vesiculation in a portion of an isolated, 2-cm length of squid giant axon in ASW at room temperature (22° C) after transection in the middle of its length is shown in Fig. 2 (similar development was observed in axons of the cephalopods mentioned in Methods). In Fig. 2A the appearance of 'blebs' is seen within 1 min after transection (at upper region of photomicrograph). In Fig. 2B, 5 min after transection, small vesicles are evident with a distribution of sizes. In Fig. 2C, 15 min after transection, some vesicles have become very large (30–50 $\mu$m) and oval shaped with 'tails' (perhaps relating to cisternal swelling, see Fig. 5A) while others are spherical. Vesicular size generally increased most rapidly in the first 30 min after transection and then slowed in the next 30 min with vesicles becoming spherical in shape and stationary.

Fig. 3 shows photomicrographs of different portions of other axon segments in ASW and at different focal planes, 30 min after each segment was cut out of an axon. Fig. 3A shows vesiculation to be extensive along the axon in a region several mm from the cut end (not shown) and at a focal plane near an inner surface of the axolemma. Also evident are clusters of vesicles and merging vesicles (20–30 $\mu$m diameter) which are indicative of vesicular fusions (Fig. 4). Figs. 3B and 3C are mid-plane views of different regions of the same axon segment. The portion of axon shown in Fig. 3B is several millimeters away from a cut end while the portion in Fig. 3C is near a cut end (lower left corner). In both portions of axon, vesicles appeared only in apposition to the axolemma, and this was invariably the case in more than 100 axons. That is, vesicle formation

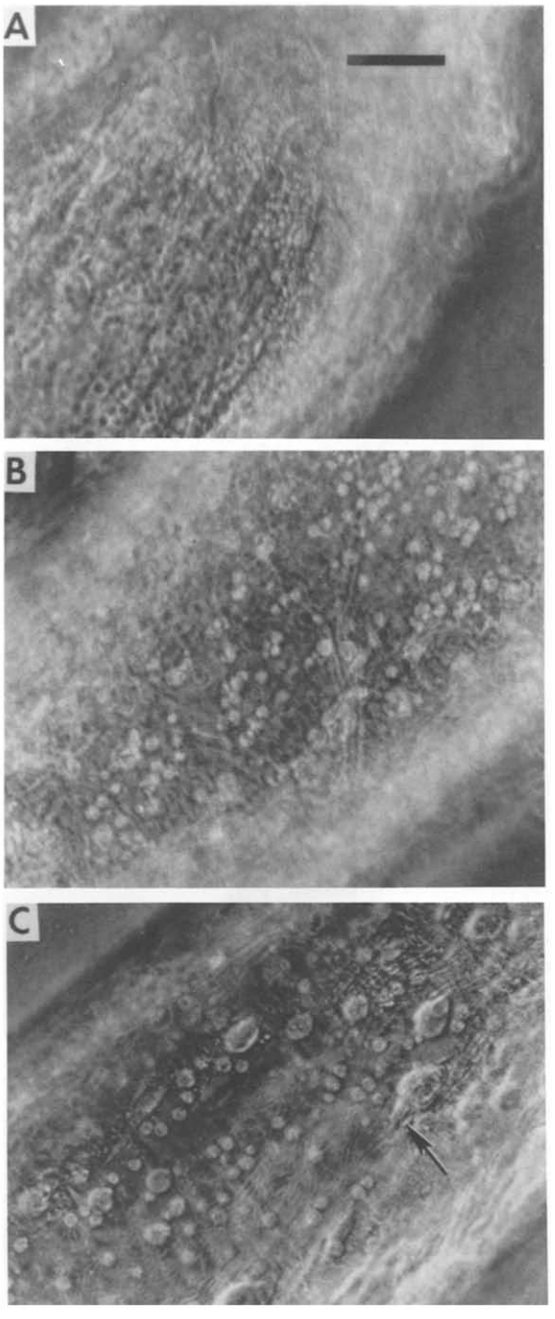


Fig. 2. Time development of vesiculation in an axon transected in ASW. (A) 1 min after transection (at top right of photo) 'blebs' and some small vesicles appear. (B) After 5 min, a distribution of vesicle sizes is evident. (C) After 15 min, some oval-shaped axosomes (large vesicles) have formed. Note the 'tail' (arrow) on some axosomes which may relate to cisternal swelling in Fig. 5. Focal plane is at an inner surface of the axolemma. Phase contrast. Scale bar 100 $\mu$m.

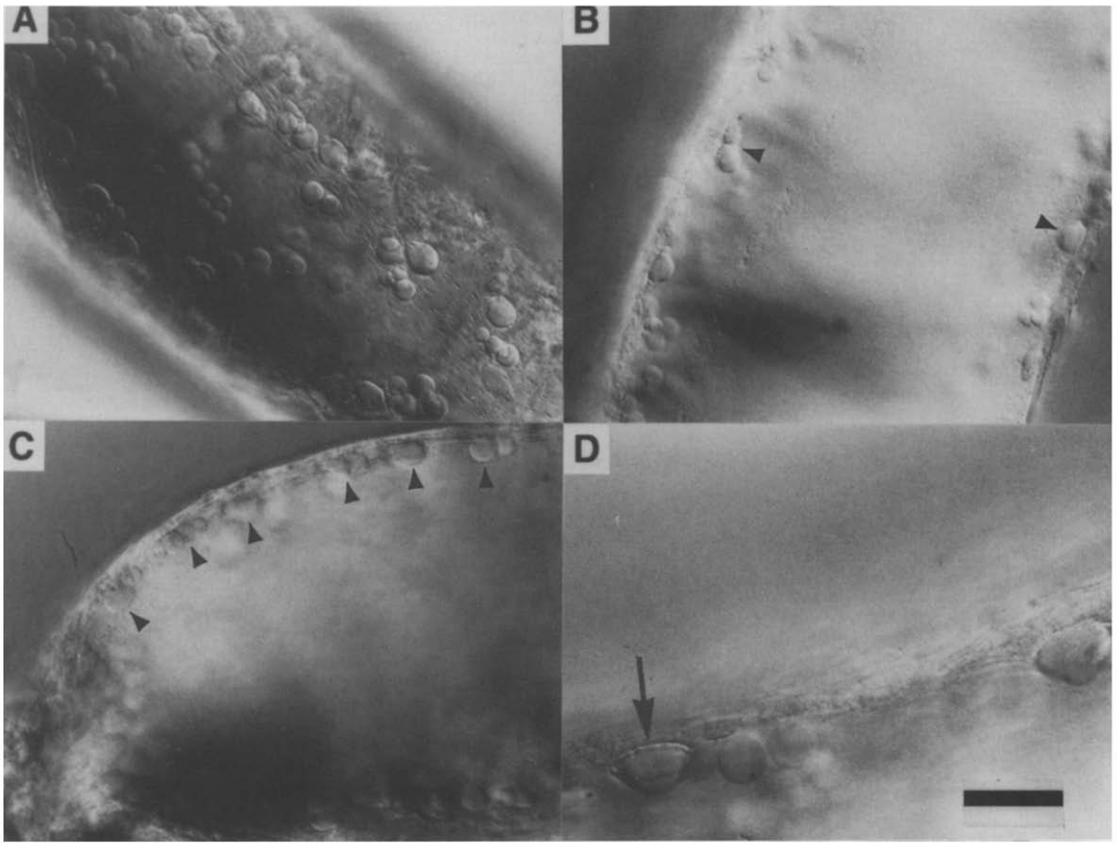


Fig. 3. Differential-interference-contrast (DIC) photomicrographs of regions of a squid axon showing vesiculation induced after transection of the axon in ASW 30 min earlier. (A) Aggregating and fusing vesicles at a focal plane near an inner surface of the axolemma. (B) A portion of axon several millimeters from the transected end in which vesicles (arrowheads) are found only in the subaxolemmal region (focal plane is at the axonal midsection). (C) The same focal plane as in (B) but in a region near the cut end (lower left corner). The vesicles (arrowheads) are again seen in apposition to the axolemma except at the constricted end, where they come together to clog the opening (see also Fig. 8). (D) Higher magnification image of the axolemmal region shows the close proximity of several vesicles to the axolemma (at the arrow tip) and one of them appears to be 'budding' inwardly (arrow), indicative of the vesiculation process. Scale bar (in (D)) corresponds to 50 μm for (D) and 100 μm for (A), (B) and (C).

occurred in the subaxolemmal region with no apparent involvement of or formation in the bulk axoplasm. In Fig. 3D, the proximity of the site of vesicle formation to the axolemma is shown at higher magnification. One subsurface vesicle is 'budding' inwardly (arrow), which is suggestive of the way in which vesiculation occurs, while others have rounded into spherical shapes.

*Possible membrane mechanisms responsible for vesiculation*

Two important facts, which bear on mechanisms responsible for vesiculation, were obtained from the previous photomicrographs. These are: the site and the extent of vesiculation. As indicated in Fig. 3, induced vesicles appear to be formed only in the subsurface vicinity of the axolemma. The mechanism responsible for vesiculation also results in a substantial amount of membrane transferred to vesicles. For example, the extent of vesiculation as determined from sterological estimates (comparing axosomal surface area to axolemmal surface area) of the total area of vesiculated membrane shown in Fig. 3A was about 20 percent of the axolemmal surface area in the same section of axon.

Based on the subsurface location of vesicles and the large amount of vesiculation, the principal membrane mechanisms that could be involved in injury-induced vesiculation are the following: (1) Endocytotic budding of axolemmal membrane in regions near the injury. (2) Local pinching off of cisterns of endoplasmic reticulum (ER) in the axon. (3) Vesiculation in burgeoning Schwann cells that erodes the axolemma, followed by merger with axonal vesicles. Evidence that all three of these mechanisms contribute to the formation of axosomes has been obtained in ultrastructural studies that will be presented elsewhere. In support of mechanism (2), the location, membrane area and function of ER are consistent with the above requirements for ER to be a source. According to Henkart et al. [17], ER contains membrane that occupies 4% of the axon volume, sufficient membrane to account for the amount of vesiculation observed, and also forms subsurface cisterns, which, in the squid axon, swell in response to

increased $Ca^{2+}$ loading [18]. Fig. 5 shows subsurface cisterns (arrows) that are swollen in an axon transected in $Ca^{2+}$-containing ASW. In addition, ER functions in regulating the amount of free $Ca^{2+}$ in axoplasm [17] to 30 nM [19]. A requirement for $Ca^{2+}$ in axosomal development is shown subsequently. Other intracellular structures, such as cytoskeletal elements and small transported vesicles from the Golgi-ER complex of the cell body, though they constitute a smaller membrane area may also be involved because organelles (granules and mitochondria) have also been shown to accumulate in regions close to axonal injury [7,20].

With respect to mechanism (3), previous ultrastructural studies of the early cytopathological changes in peripheral myelinated nerve injured by transection showed expansion of Schwann cell cytoplasm and erosion of axolemma until incursion of the Schwann organelles into the axon and commingling with axonal organelles [6]. Thus, Singer and Steinberg [6] concluded that the Schwann cell response in transected nerve plays a principal role in axon degeneration.

*Vesicular fusion and movement within an axon*

In Fig. 3A vesicles are aggregating and many vesicles

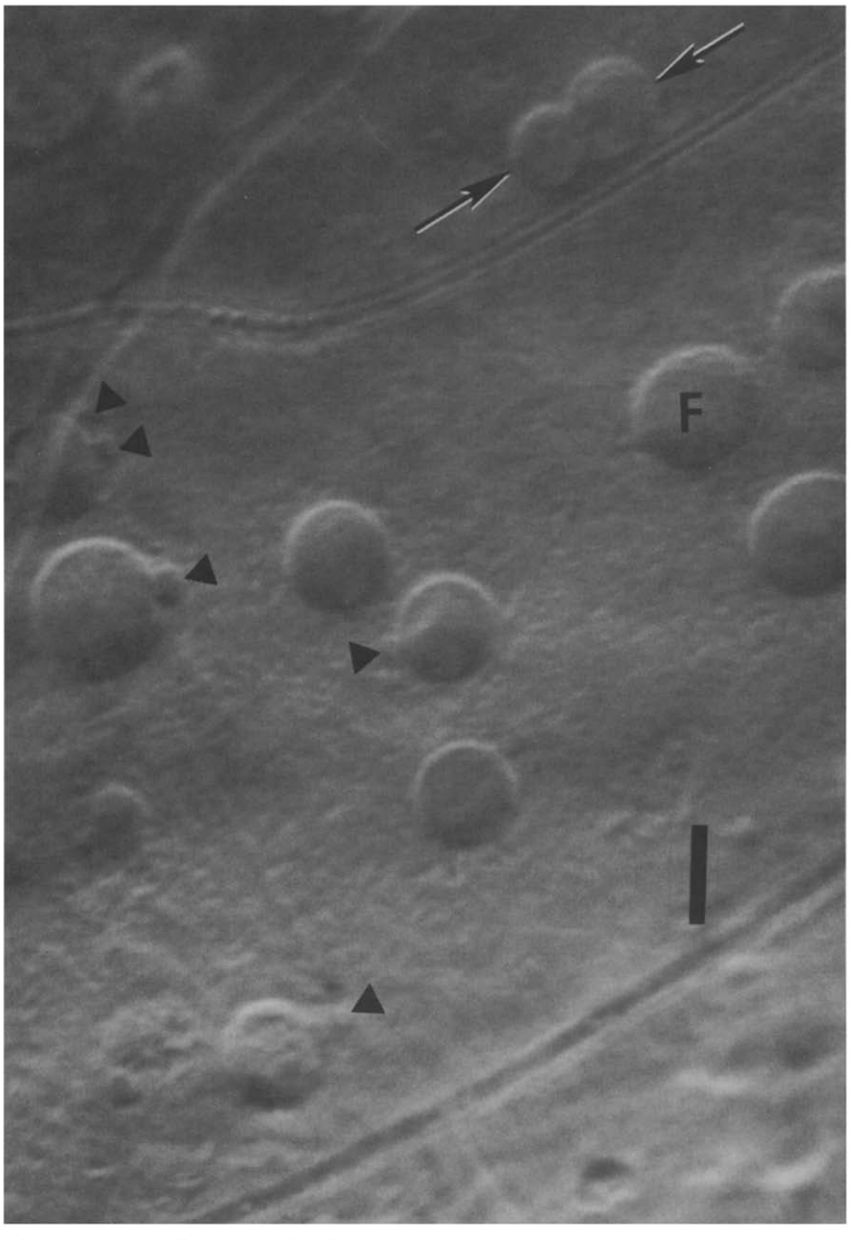


Fig. 4. Vesicular fusions with axosomes. Small vesicles (triangles) appear to be incorporated into axosomes, suggesting that axosomes are mosaic membranes from different sources. Partly fused axosomes (between arrows) and an almost completely fused pair of axosomes ('F'). Phase contrast. Scale bar 25 $\mu$m.

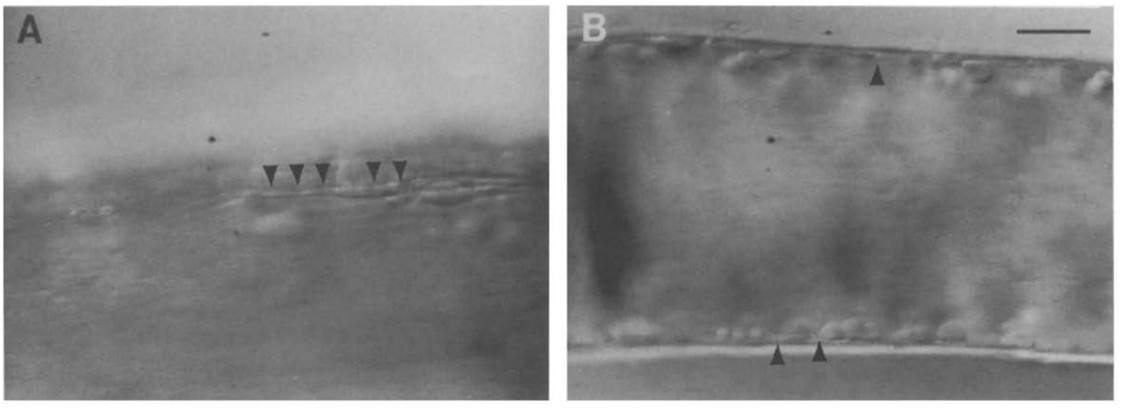


Fig. 5. Subsurface, swollen cisterns and connected tubes associated with injury-induced vesiculation. (A) Arrowheads mark a long tube connecting several vesicles. (B) The proximity of the cisterns (arrowheads) and vesicles to the axolemma. DIC. Scale bar in (B) 100 μm, for (A) 50 μm.

have the appearance of melding into one another (Fig. 4), which suggests that axosomal enlargement occurs by vesicular fusions. A clear example of axosomal movement and an increase in vesicle size, apparently due to fusion, is shown in Fig. 6. An irregularly-shaped axosome, labeled 'A', (arrow) is seen in Fig. 6A. In another photomicrograph, Fig. 6B, of the same section of axon, 7 min later, the shape of the axosome has changed and its area has increased (suggesting that fusion has occurred) and the position of the axosome has changed, indicating movement (at a rate of about 20 μm/min) of the axosome toward the cut end (below the left corner of photo). The appearance of several other large vesicles in Fig. 6B that are not evident in Fig. 6A is also consistent with fusion and movement of vesicles. Axosomal movement was always toward a site of injury. Thus, when an axon was partially cut but not transected, axosomes were observed moving toward the injured site on both sides of a longitudinal plane normal to the hole. In light of known rates of axoplasmic transport of organelles and large macromolecules [21], the rate of movement of these large vesicles is comparable and suggests a translocation mechanism.

Confirmation of fusion events between vesicles was obtained directly in continuous recordings of vesicular movements in 'real time' by video DIC-microscopy [11]. Fig. 7 shows a sequence of photomicrographs, taken from video tape, from which the fusion of two axosomes (arrowheads) near the transected end of an axon in ASW is evident. In Fig. 7A the two axosomes have just begun to come together. Less than 1 s later (Fig. 7B), the two axosomes are still recognizable as individual

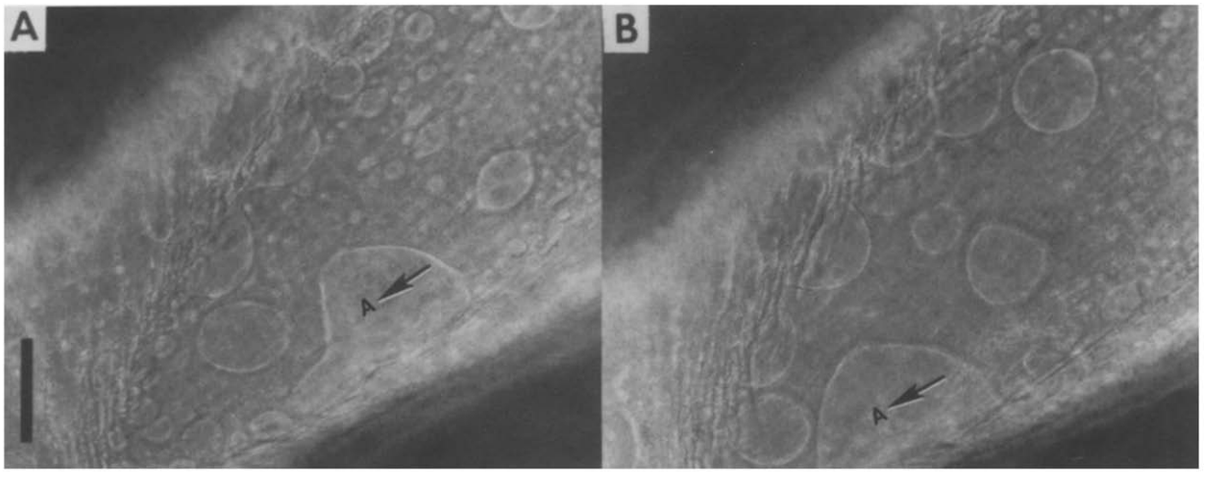


Fig. 6. Axosomal movement and fusion in an axon transected in ASW. (A) A large irregularly-shaped axosome 'A' (arrow) before fusion. (B) 7 min later, the same axosome has changed shape and increased in area, apparently due to fusion, and has moved toward the cut end (not shown) in the direction of the arrow. The rate of movement was calculated to be about 20 μm/min, which is suggestive of a translocation mechanism [21]. The time development of two fusing axosomes is shown in Fig. 7. Note other axosomal size increases and movements during the elapsed time from (A) to (B). Phase contrast. Scale bar is 100 μm.

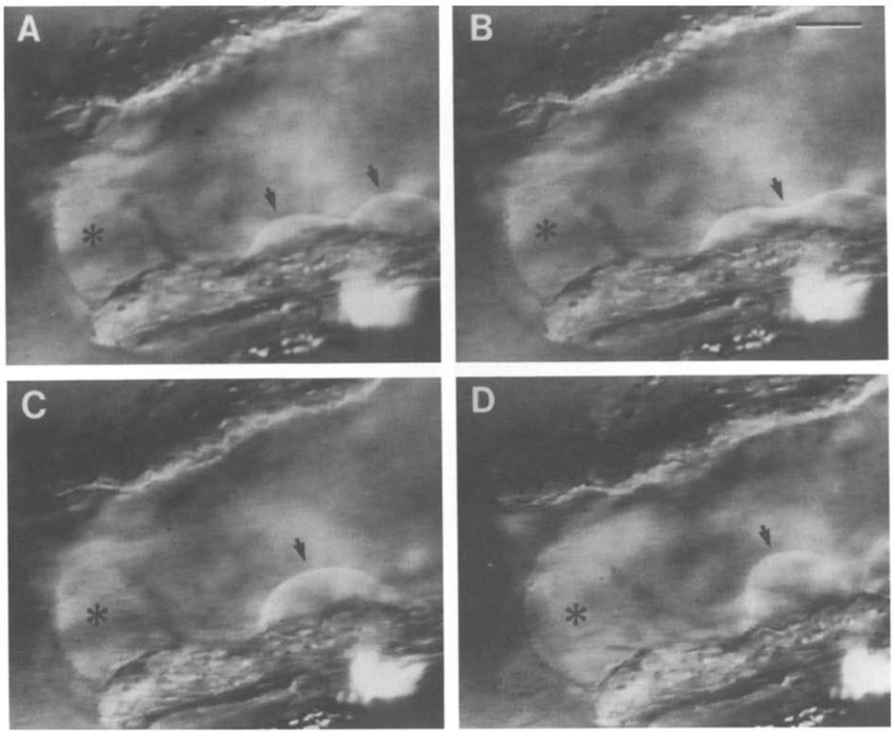


Fig. 7. Sequence of micrographs from video tape showing fusion of two axosomes near a cut end of an axon (mid-plane focus) transected in ASW. (A) The onset of fusion as the two axosomes (arrowheads) come together. (B) Less than 1 s after (A) fusion has progressed. Two distinct axosomes are still discernible. (C) The axosomes have merged into a single entity 1 min later. (D) 5 min elapsed time from (A), the united axosomes have rounded in shape and moved toward the cut end. Notice the large axosome (asterisk), located at the cut end, that spans the opening of the constricted cut end. DIC. Scale bar in (B) is 100 $\mu$m.

merging entities. In Fig. 7C, 30 s after the onset of fusion, fusion is completed and only one axosome with an elongated shape is seen. Finally, in Fig. 7D after an elapsed time of a few minutes, the united axosome became rounded in shape and moved closer to the cut end.

*Membrane redistribution and occlusion of a cut end*

In transected squid giant axons the cut ends constrict [2]. Although the constriction was previously thought to be sufficient to allow reestablishment of a barrier between the axon interior and the external medium, we also observed occlusion by axosomes. Fig. 8A shows the

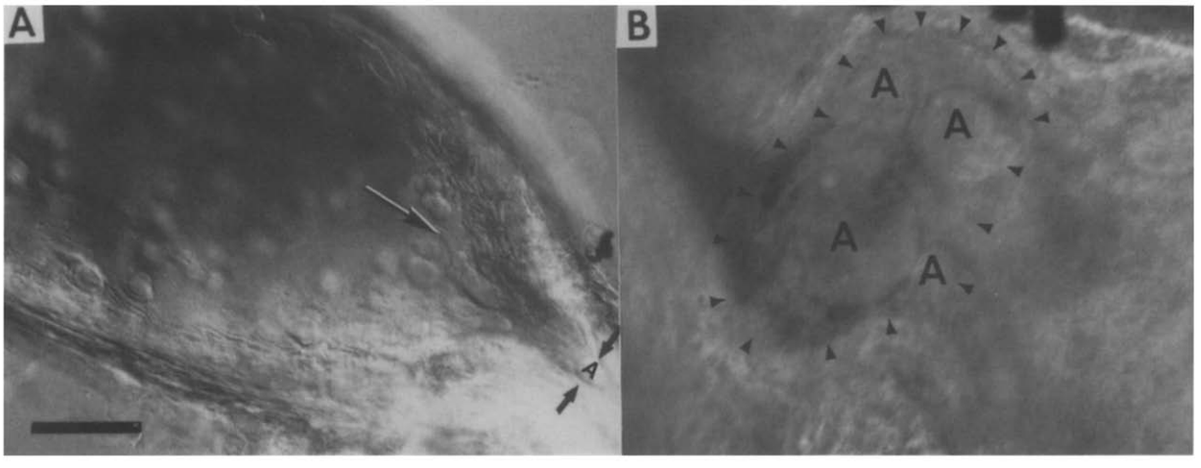


Fig. 8. Axosomal accumulation and occlusion at a constricted cut end of an axon. (A) The constricted passage (direction of large arrow) of a transected axon 30 min after cutting in ASW with an axosome 'A' (between the small pair of arrows) obstructing the narrowed passage. Other axosomes appear to be 'flowing' into the narrowed passage. (B) An axial view of the constricted cut end of another axon with axosomes (labeled 'A') occluding the cut opening (marked by arrowheads) of the axon (oriented to the right). These observations suggest a role for axosomes in reestablishing a barrier between the inside and outside of an axon. Phase contrast. Scale bar in (A) is 100 $\mu$m for (A) and 50 $\mu$m for (B).

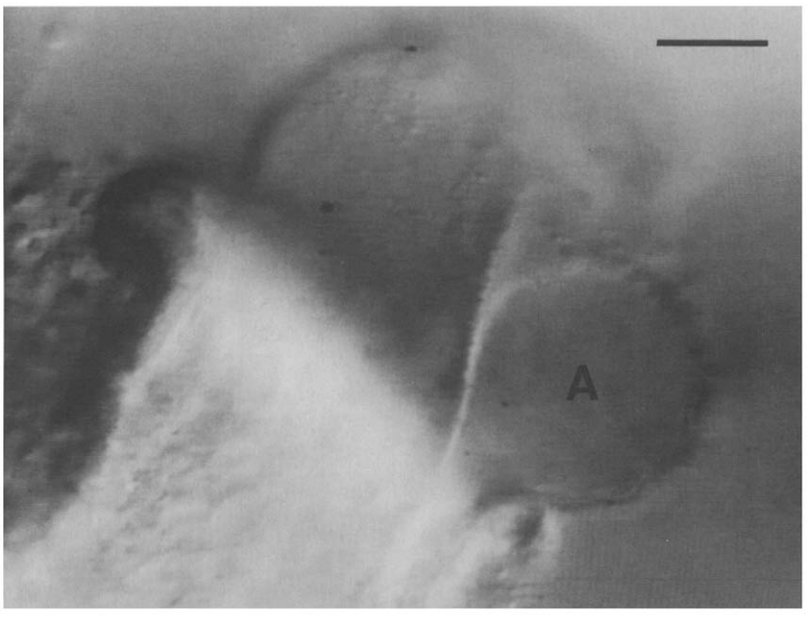


Fig. 9. Emergence of a giant axosome 'A' from a transected end of an axon (similar to that following the movement of an axosome out of the cut end of an axon illustrated in Fig. 10). Notice the rounded shape compared to the shape during movement inside an axon (Fig. 10) and the 'cloud' of cytoskeletal debris. DIC. Scale bar is 100 $\mu$m.

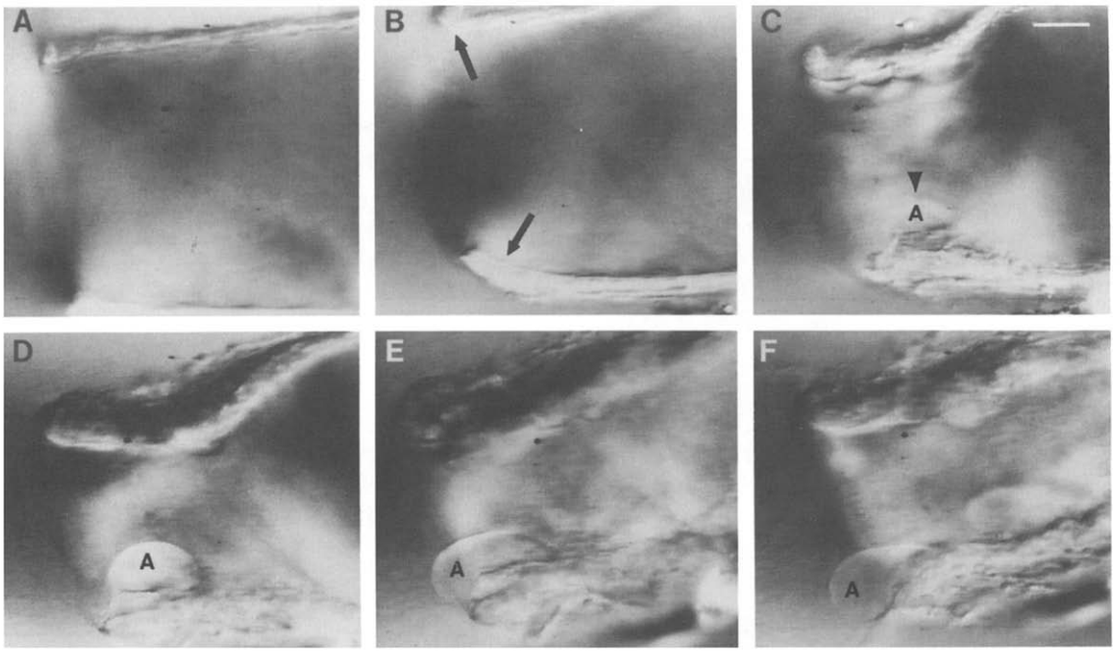


Fig. 10. $Ca^{2+}$-induced axosomal formation and movement after transection of a squid giant axon in divalent-cation-free (DCF) ASW and addition of 10 mM $Ca^{2+}$ to the DCF-ASW bath. (A) Cut end of axon 15 min after transection in DCF-ASW. The end remained open, as shown, as long as the external solution was divalent-cation free. (B) 1 min after $Ca^{2+}$ was added to the DCF-ASW, bringing the bath $Ca^{2+}$ concentration to 10 mM. The cut end began to constrict, as indicated (arrows) in (B). (C) At 3 min, the constriction of the end was more pronounced and an axosome 'A' (arrowhead) had already formed at the lower internal surface of the constricted opening. (D) At 6 min, further constriction had occurred and axosome 'A' had develoed into a large ellipsoidal ball. (E) At 15 min, axosome 'A' had changed shape and moved into the opening. (F) At 20 min, axosome 'A', resembling a 'tear drop', had moved partially out of the opening. Substitution of $Mg^{2+}$ for $Ca^{2+}$ in other experiments of this type yielded similar results but 50 mM $Mg^{2+}$ was required to produce the same extent of vesiculation as 10 mM $Ca^{2+}$. This sequence of photographs was reproduced from video tape [11]. The process illustrated in this figure continued with the emergence of axosome 'A' and other axosomes from the cut end. Once out of the axon, axosomal shape became that of large spheres, as in Figs. 9 and 11. DIC. Scale bar in (C) is 100 $\mu$m and applies to (A), (B), (D) and (E) also.

constricted end of a transected axon in which migrating axosomes accumulate and are forced together, clogging the passage. One axosome is seen (labeled 'A' between the pair of arrows) occluding the narrowed passage. In Fig. 8B, a view of a constricted opening (marked by arrowheads) of another cut axon shows several large axosomes in direct contact and occluding the opening. These observations suggest that axosomes could be involved in reestablishing a barrier at the transected end.

Further evidence in support of this suggestion is shown in Fig. 7 in which a large axosome (marked by an asterisk) located at the opening of a cut axon developed with time (not shown) in an apparent attempt to fill the opening. To form a seal, axosomes, in addition to spanning the opening, must also fuse with the axolemma. Axosomal fusion with the disrupted axolemma at the cut end seems possible because emerging axosomes were generally larger than those within an axon (compare the size of the emerging axosome in Fig. 9 with those within an axon in previous figures), suggesting that axosomes readily come in contact and fuse with one another as they pass through a constricted cut end. Such fusions were observed.

*Divalent cations are required for vesiculation*

A requirement for divalent cations in the constriction process that narrows the opening at the ends of a transected squid axon has recently been demonstrated [2] and a similar requisite for sealing of transected cockroach axons has also been reported [3]. Axosomal formation also requires divalent cations, as illustrated in the sequence of micrographs taken from videotape and shown in Fig. 10. An axon was transected in divalent-cation-free ASW, and Fig. 10A shows its condition after 15 min. The transected end is open and no axosomes are evident; generally, axosomal formation did not occur in divalent-cation-free ASW. Upon addition of $Ca^{2+}$ (10 mM) to the bath, the end immediately began to constrict, as seen 1 min later in Fig. 10B (arrows). In Fig. 10C, at 3 min, the end constricted further and the presence of an axosome (arrow) is evident. In Fig. 10D, 6 min after addition of $Ca^{2+}$, both processes advanced

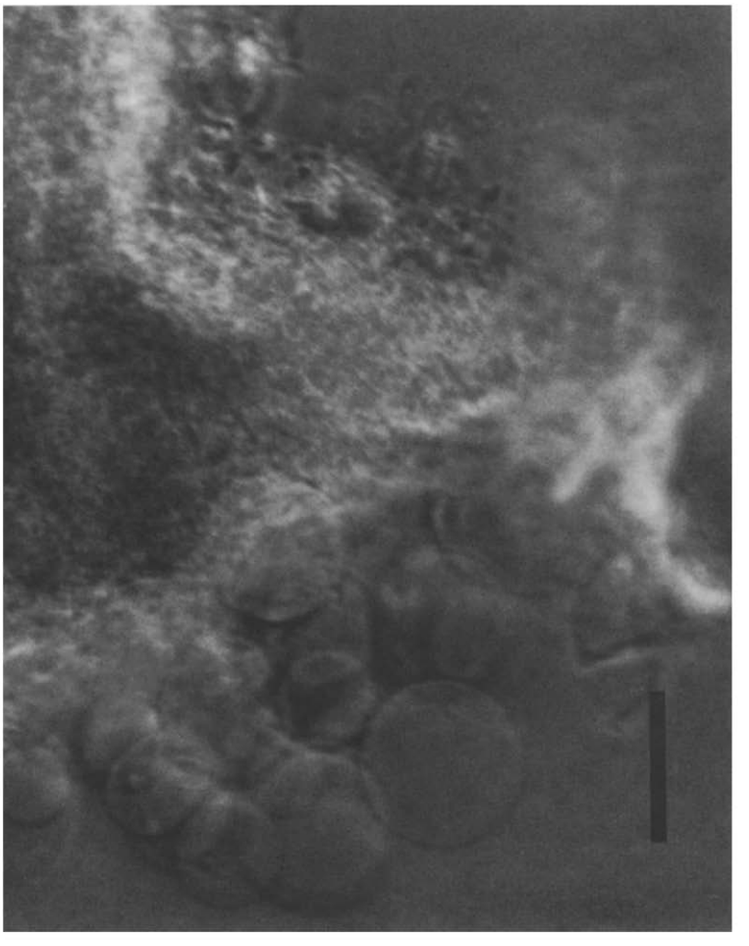

Fig. 11. Axosomes spontaneously liberated from a cut end of a squid axon 30 min after transection in ASW. On emerging from a cut end axosomes were usually covered with cytoskeletal debris, as in Fig. 9. However, with time, some axosomes drifted out of the debris while remaining attached to it, as shown here. Axosomes such as those in this figure were stable for many hours and many membrane patches could be excised from them for patch clamp measurements of ion channels, as shown in subsequent figures. Phase contrast. Scale bar is 100 $\mu$m.

and the axosome increased in size. In Figs. 10E and 10F after 15 and 20 min, respectively, the axosome continued to grow but also became mobile, moving out of the cut end in the shape of a 'tear drop', but rounding into a spherical shape, as in Fig. 9, once out of the axon. Eventually, a sufficient number of axosomes arrived at the constricted opening to occlude it (see Fig. 8). $Mg^{2+}$ (50 mM) added to a divalent-free bath solution also induced axosomal formation to the same extent as 10 mM $Ca^{2+}$ in cut axons (axoplasmic free $Mg^{2+}$ concentration is normally about 3 mM [22]). Thus, to obtain axosomal formation after axonal transection divalent cations ($Ca^{2+}$ or $Mg^{2+}$) were required in the external solution. Furthermore, a synergistic effect of $Na^+$, $Cl^-$, $Ca^{2+}$, and $Mg^{2+}$ in ASW was observed in that the extent of axosomal formation was always less than that produced in ASW if $Cl^-$ was replaced by glutamate, if $Na^+$ was replaced by $K^+$ or if one of the divalent cations was omitted. Thus all of the major constituent ions in ASW (and also in squid blood) promote vesiculation in transected axons. By comparison, if the external solution in which axons were transected contained increasing amounts of the principal ionic constituents found in axoplasm (e.g., $K^+$, taurine, glutamate and glycine) vesiculation in transected axons was reduced or prevented. These observations are similar to those reported for constriction of the cytoskeleton at a cut end of a squid axon [2].

*Axosomes contain ion channels*

As inferred from Fig. 9, in their passage through a constricted, open end of a cut axon, some axosomes fuse and consequently emerge from an axon much larger in size (maximum observed, 250 $\mu$m diameter) than ones (Fig. 3A) within an axon. The attachment of axosomes to protruding axoplasm provided a stable anchor that allowed access to their surfaces and isolation of a patch by an electrolyte-filled glass pipet. Electrical isolation, of about 100 gigohms, of patches of the external surface of an axosome and the subsequent recording of ion channel current demonstrated the membranous structure of axosomes.

Fig. 11 shows an axosome of about 100 $\mu$m diameter, outside the cut end of an axon, from which a patch was isolated, excised and voltage clamped. Current records (Fig. 12) were obtained seconds after establishment of the constant potentials indicated (pipet voltage relative to bath voltage). The representative sample records on

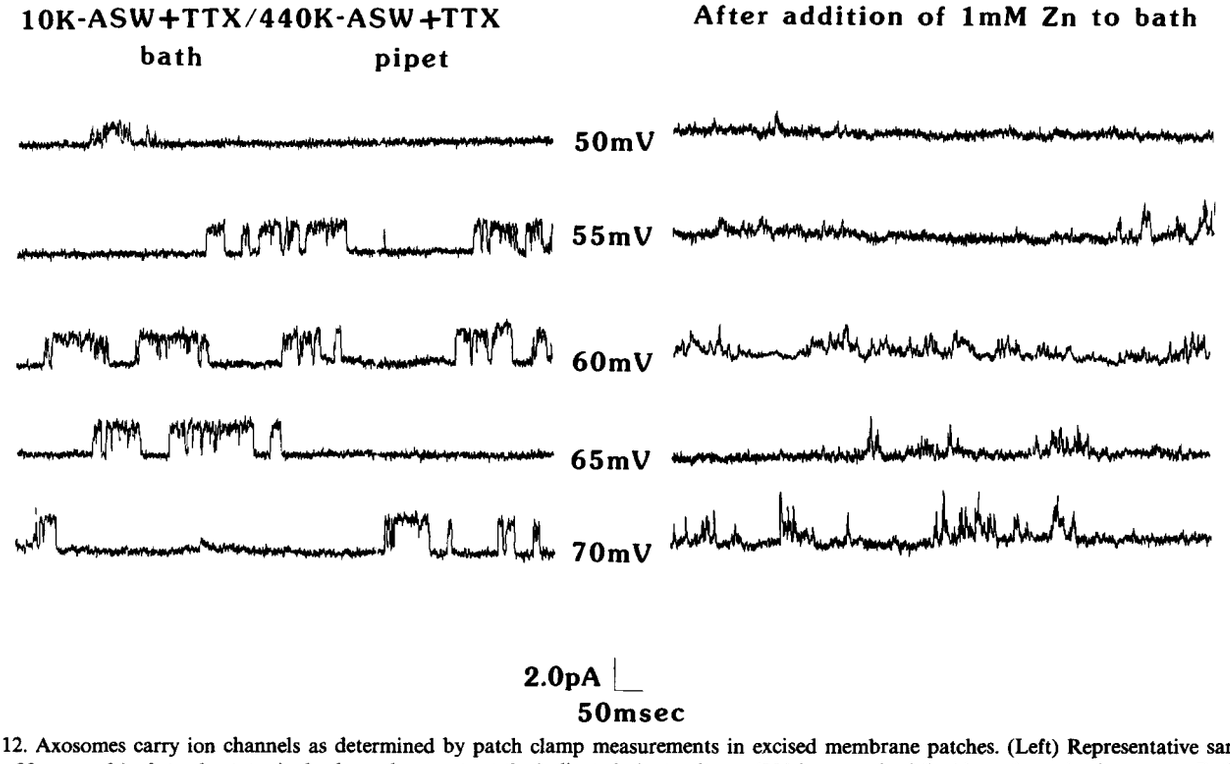


Fig. 12. Axosomes carry ion channels as determined by patch clamp measurements in excised membrane patches. (Left) Representative samples (from 20-s records) of steady-state single-channel currents at the indicated pipet voltages ($V_p$) in an excised (inside-out) patch of axosome. Bath and pipet solutions contained 1 $\mu$M TTX to eliminate conduction in voltage-sensitive $Na^+$ channels. Substitution of glutamate for chloride produced no significance changes (in either conductance or kinetics) in the current records shown on the left side. Addition of TEA (50 mM) and 3,4-DAP (1 mM), known blockers of axolemmal $K^+$ channels, to both bath and pipet solutions did not affect this channel. (Right) Sample records from the same excised patch as recorded left and at the same potentials after addition of 1 mM $Zn^{2+}$ to the bath solution. $Zn^{2+}$ (1 mM) affects axolemmal $K^+$ conductance activation kinetics in squid axon [14,15] and, as indicated in the above records, altered the kinetics of channel openings at the same voltages. Channel openings (conduction) are upward deflections from baseline (no conduction) that correspond to current flow out of the pipet directed into an axosome. Bath temperature was 24° C.

the left half of Fig. 12, taken from longer duration (20 s) current records, show a noisy, binary waveform with random transitions characteristic of the opening (upward deflections) and closing of a single channel. Analysis of the entire 20-s length records, at the potentials shown in Fig. 12 and at additional potentials (not shown in Fig. 12), yielded the essentially bimodal amplitude histograms graphed in Fig. 13. The largest of the two peaks in Fig. 13 corresponds to the nonconducting state (baseline of records in Fig. 12) and the other peak to the single conducting state. The bimodal distribution of current states (one of which corresponds to no conduction) at each voltage indicates that these current recordings are from a single channel. The horizontal

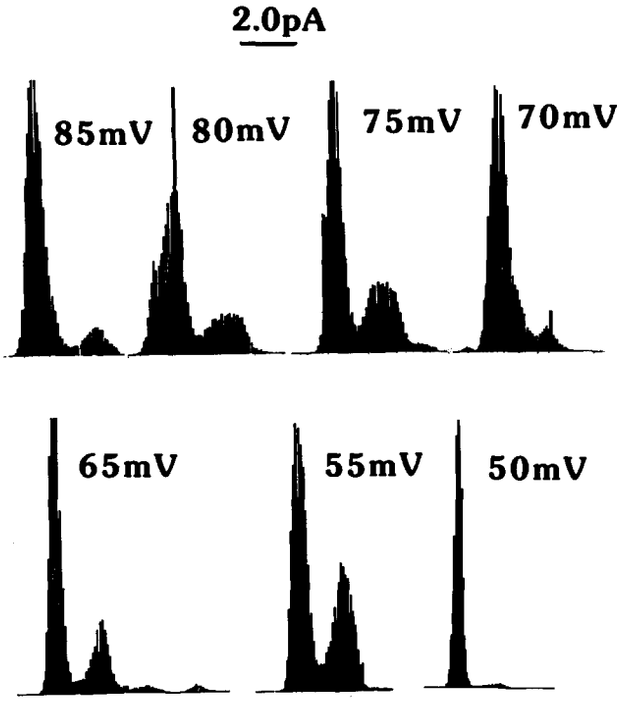


Fig. 13. Amplitude histograms produced from the entire length (65 536 points) of single-channel records, shown partially in Fig. 12 (left), and from additional records at other potentials in the same patch. The ordinate corresponds to the number of occurrences of each current amplitude in each record and the abscissa is current amplitude. The origin of each histogram corresponds to zero units for both ordinate and abscissa. The bimodal distribution indicates that the recorded current waveform for this channel at each voltage was composed of two distinct levels (reflecting either no conduction or conduction). The largest peak in each histogram corresponds to the nonconducting channel state (baseline of records in Fig. 12). The peak value of the linear ordinate (in number of occurrences of a current amplitude in a single-channel record) at each voltage is as follows: 50 mV (9000), 55 mV (3000), 65 mV (3440), 70 mV (5600), 75 mV (3400), 80 mV (2368) and 85 mV (6800). The 2 pA scale bar above the figure applies to the linear abscissa in all histograms. The horizontal displacement (current) between the predominant two peaks was taken as the single-channel current at each patch voltage to obtain the current-voltage relation in Fig. 14. The open probability of the first current level above baseline at each voltage was calculated to be: 50 mV (0.10), 55 mV (0.29), 65 mV (0.32), 70 mV (0.20), 75 mV (0.37), 80 mV (0.23), 85 mV (0.35).

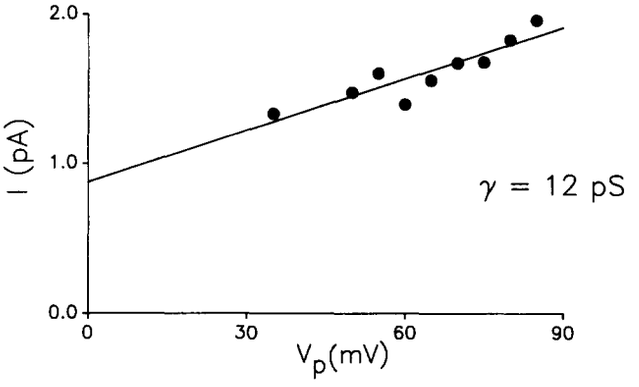


Fig. 14. Single-channel current-voltage, $I(V_p)$, plot derived from the data of Figs. 12 and 13. The straight line is the best linear regression through the data points. Data for potentials less than 30 mV were not obtained because of the activity of other channel types which resulted in complicated waveforms. While the $I(V_p)$ relation in highly asymmetrical potassium solutions is expected to be nonlinear the linear extrapolation provides an approximation of the reversal potential (−80 mV) of this channel and the slope gives an estimate of the conductance (12 pS). The only ion gradient under the conditions of measurement that is close to the approximate reversal potential is that of potassium ($E_K = -97$ mV, $E_{Ca} = 0$, $E_{Cl} = 0$, $E_{Na} \gg 0$). These data and the previous results eliminating a chloride channel together with the effect of $Zn^{2+}$ on channel kinetics suggest a potassium channel.

difference (current) between the estimated peaks (most frequently occurring values) in the histogram at each potential was then taken to be the steady-state, single-channel current, $I$, which yielded the single-channel current-voltage, $I(V_p)$, data in Fig. 14. The straight line drawn in Fig. 14 is the best linear regression through all of the data points and has a slope of 12 pS. The same procedure was applied to data from two other excised patches yielding single-channel conductances (slopes) of 11.5 and 13 pS.

Because of the presence in these patches of other channel types which became active at patch potentials less than 30 mV, $I(V_p)$ data over a wider voltage range could not be obtained. Consequently, the shape of the single-channel $I(V_p)$ relation and the reversal potential of the channel remain undetermined. Nevertheless, an estimate of the reversal potential extrapolated from a linear fit of the data in Fig. 14 yields a large negative value (−80 mV) which, given the experimental ion concentration gradients (bath: 10 mM $K^+$, 430 mM $Na^+$ pipet: 440 mM $K^+$, trace amounts of $Na^+$), is consistent only with that for potassium ($E_K = -97$ mV, $E_{Na} \gg 0$). The extrapolated reversal potential is only approximate because the $I(V_p)$ relation is probably nonlinear for asymmetrical $K^+$ solutions. In such a case the slope of the linear regression through the data points at large depolarizations is taken as an estimate of the open, single-channel conductance.

Substitution of glutamate for chloride in both pipet and bath solutions yielded similar single-channel con-

ductances; demonstrating that these data are not from a chloride channel. A voltage-sensitive sodium channel is excluded because TTX was present in both solutions and, as indicated above, the channel reversal potential is inconsistent with the experimental $E_{Na}$. The conductance obtained from the slope of the best linear fit of the single-channel $I(V_p)$ data is in the range of estimates (2–12 pS) for potassium channels in the axolemma of squid axon, as previously demonstrated by spectral analyses of fluctuations measured from large populations of channels [23,24]. The slope conductance is also close to the 10 pS value reported recently in patches of cut-open squid axon, following exposure to $K^+$-free ASW [25].

Substances known to blockade $K^+$ channels in the axolemma of squid axons were applied to the channel described in Figs. 12–14. Neither TEA (50 mM) nor 3,4-DAP (1 mM) when added to either bath or pipet solutions had any obvious effect on single-channel recordings. However, addition of 1 mM $Zn^{2+}$ to the bath (Fig. 12, right side records) of the same excised patch, with control records at the same potentials on the left side of Fig. 12, severely altered channel openings, which became 'spikey' and shorter in duration. Millimolar concentrations of $Zn^{2+}$ when internally perfusing or when in the ASW bathing an axon has been shown to slow $K^+$ conductance activation (on) kinetics in voltage clamp experiments [14,15]. The $Zn^{2+}$ effect on the single channel currents in Fig. 12 is consistent with these previous findings of altered potassium channel kinetics. Thus, all of the above data taken together indicate a potassium channel, the relationship of which to axolemmal potassium channels remains to be resolved. A $Ca^{2+}$ channel [26] and another channel with multiple conducting states and larger conductances were also observed (to be reported elsewhere) under different ionic conditions.

## Discussion

Although early (less than an hour) vesiculation of injured nerve has been observed previously in other preparations [3,27], the circumstances involved in initiation and formation of vesicles after injury has not been described. Historically, the squid giant axon preparation has enabled observation of phenomena not easily observed in other axonal preparations. The giant axon preparation allowed implementation of real-time observations in functional axons. These observations suggest that injury-induced vesiculation, fusion and membrane redistribution are a direct consequence of the entry of specific ions ($Ca^{2+}$ and $Mg^{2+}$) from the external medium into the interior of an axon.

Several previous works demonstrated the effect of different ions in the axoplasm of squid axon on axonal function. Tasaki and co-workers [4,5] examined the detrimental effect of various ions in the perfusate of internally perfused axons on electrical excitability. They showed that the survival time of axons internally perfused with buffered $K_2SO_4$ solutions containing $Ca^{2+}$ (10 mM) was reduced to about 15 min. $Ca^{2+}$ was also shown to be 5-times more effective than $Mg^{2+}$ (50 mM) in reducing survivability. Although a relationship between injury-induced vesiculation and axolemmal survivability was not determined in our experiments, the similarity of the effect produced by $Ca^{2+}$ and $Mg^{2+}$ at the same concentrations (10 and 50 mM, respectively) and in a similar time interval (15 min) suggest a connection. Furthermore, axonal survival time for various $K^+$-salt solutions of univalent anions followed the lyotropic series of protein chemistry and survival time in $K^+$ solutions was much better than in $Na^+$ solutions [5]. These univalent ion effects on axon excitability are also consistent with our observations on the relative effectiveness in inducing vesiculation of the various ions ($Na^+ > K^+$, $Cl^- >$ glutamate) in the external solution bathing transected axons.

A closer association exists between injury-induced vesiculation and previously observed changes in axonal cytoskeleton. After internal perfusion with $Ca^{2+}$-containing solutions, Metuzals and Tasaki [28] showed that the ultrastructure of a squid axon contained rugged, clusters of grape-like structures on the inner aspect of the axolemma, which was devoid of a normal subaxolemmal filamentous network. More recently, after internal perfusion of squid axon with a KCl solution for 1 h, scanning electron micrographs showed a disrupted cytoskeleton and vesicles appeared on the internal surface of the axolemma (which was excitable up to the moment of fixation) [29]. Thus, ionic conditions that produce a disruption of the cytoskeleton also produce injury-induced vesiculation. Furthermore, the role of calcium in activating proteases within squid axon [30,31] and in other cells [32] is recognized in membrane cytoskeletal interactions [33] as is the requirement of calcium and magnesium in membrane fusion processes [34].

Injury-induced vesiculation and membrane redistribution seem to be processes associated either with neural degeneration or with neural repair. Repair is possible if transected squid giant axons can regenerate. Presently, the answer to this question is unknown. Nevertheless, transected cockroach axons are able to seal rapidly (1 h) [3] and regenerate after several days [35]. In addition, in cockroach axons 'vacuoles', similar to the vesicles reported here, are also seen in conjunction with a partition-like structure, presumed to be the seal [3]. Thus, the squid axon may have a mechanism for repair regardless of whether or not axons can regenerate. In degeneration, vesiculation could be a manifestation of the degradation of axonal structures by $Ca^{2+}$-activated enzymes. In this respect, the role of Schwann cells in axonal destruction, as described in vertebrate

nerve [6], could be relevant. In repair, divalent cations could activate fusion-promoting enzymes [34] and axosomes could provide the structures necessary to seal a cut axon. In addition, as demonstrated in Fig. 12 and in Ref. 26, axosomes carry ion channels that could play a role in the recovery process, such as enhancement of the $Ca^{2+}$ concentration in the growth cone of regenerating neurons [35–38], after axosomal incorporation into the seal. Sealing after injury also occurs in cardiac muscle [39] and in skeletal muscle [40] fibers bathed in high $Ca^{2+}$ solutions.

Intracellular vacuolarization is found in many neurodegenerative diseases such as Creutzfeldt-Jakob's and Alzheimer's disease. The cause of these diseases remains unknown, but evidence suggests [41] that membrane damage is a primary event preceding the appearance of amyloid protein deposition in the brain, which is considered a precursor of Alzheimer's disease. Vesiculation induced by injury may also be a manifestation of the same process that gives rise to subaxolemmal 'vacuolar degeneration' seen during peripheral neuropathy associated with demyelination of axons in mutant hamster [42] and in murine motor neuron disease of the central nervous system [43]. Both of these disorders involve a redistribution of axonal cytoskeleton (similar to that described in this article) and axonal organelles in myelinated nerve fibers. Thus, injury-induced vesiculation in squid giant axons may be a useful model for study of neurodegenerative processes.

The patch clamp measurements of channels in excised patches from axosomes gave values for open-channel conductance and estimated reversal potential and an effect of $Zn^{2+}$ that indicates a $K^+$ channel. However, this channel was unaffected by the usual $K^+$-channel blockers, TEA and 3,4-DAP. This latter result could mean that the channel is not an axolemmal $K^+$ channel, one that is a precursor of an axolemmal channel with different structural properties or a channel whose sites of affinity for TEA and 3,4-DAP have been altered in the mosaic axosomal membrane. Nevertheless, the important result with respect to these experiments is the demonstration that axosomes carry ion channels. Thus, the results presented here demonstrate not only the redistribution of membrane but redistribution of ion channels too, following injury. As suggested earlier, channels redistributed via axosomal incorporation into a seal could have a role in regenerating neurons.

Membrane vesicles containing ion channels have been prepared previously from a variety of cell preparations. For example, a droplet of extruded cytoplasm from the plant cell *Nitella* was first introduced in 1957 [44]. Membrane blebbing was achieved in several preparations [45–48] by treatment with vesiculation-inducing agents in conjunction with enzymatic treatment. Recently, blebbing of native sarcoplasmic reticulum (sarcoballs) from skeletal muscle fibers was achieved without enzymatic treatment by skinning the fibers in $Ca^{2+}$-containing saline solution [49]. Axosomes follow this line of development in which vesicles are derived from cell preparations but, as in the production of sarcoballs, do not require use of enzymes or exogenous vesiculating agents. Because axosomes are likely to be composed of membrane from inaccessible intracellular sources and are amenable to many different techniques and because they are produced with ease in large quantities and sizes, they may be useful in the study of ion channels or other membrane processes.

## Acknowledgements

We thank H.R. Leuchtag, L., Reuss, A. Ritchie and G. Szabo for comments on the manuscript. We also thank Roger T. Hanlon of the Marine Biomedical Institute in Galveston for supplying cephalopods through NIH grant RR01024, the Marine Biological Laboratory in Woods Hole for the use of facilities and Philip Presley and Carl Zeiss Inc. for the use of equipment. Supported by ONR Contract N00014-87-K-0055 (H.M.F.) and done during the tenure of a Grant-in-Aid award from the American Heart Association and Wyeth-Ayerst Laboratories (P.G.S.).

## References

1 Smythies, J.R. (1971) Int. Rev. Neurobiol. 14, 49–124.
2 Gallant, P.E. (1988) J. Neurosci. 8, 1479–1484.
3 Yawo, H. and Kuno, M. (1985) J. Neurosci. 5, 1626–1632.
4 Tasaki, I., Watanabe, A. and Takenaka, T. (1962) Proc. Natl. Acad. Sci. USA 48, 1177–1184.
5 Tasaki, I., Singer, I. and Takenaka, T. (1965) J. Gen. Physiol. 48, 1095–1123.
6 Singer, M. and Steinberg, M.C. (1972) Am. J. Anat. 133, 51–84.
7 Zelena, J., Lubinska, L. and Gutmann, E. (1968) Z. Zellforsch. Microsk. Anat. 91, 200–219.
8 Hamill, O.P., Marty, A., Neher, E., Sakmann, B. and Sigworth, F. (1981) Pflügers Arch. 391, 85–100.
9 Stein, P.G., Fishman, H.M. and Tewari, K.P. (1989) Biophys. J. 55, 588a.
10 Fishman, H.M., Stein, P.G. and Tewari, K.P. (1989) Biophys. J. 55, 588a.
11 Tewari, K.P., Stein, P.G. and Fishman, H.M. (1989) Biophys. J. 55, 171a.
12 Fishman, H.M., Tewari, K.P. and Stein, P.G. (1989) Soc. Neurosci. Abstr. 15, 160.
13 Arnold, J.M., Summers, W.C. and Gilbert, D.L. (1974) A Guide to the Laboratory Use of the Squid *Loligo pealei*, pp. 61–64, Marine Biol. Lab. Woods Hole.
14 Begenisich, T. and Lynch, C. (1974) J. Gen. Physiol. 63, 675–689.
15 Gilly, W.M. and Armstrong, C.M. (1982) J. Gen. Physiol. 79, 965–996.
16 Fishman, H.M. and Law, W.C., Jr. (1987) Proc. 9th Annu. Conf. Inst. Elect. Electr. Engr. Engineering in Medicine and Biology Society 2, 460–461.
17 Henkart, M.P., Reese, T.S. and Brinley, F.J., Jr. (1978) Science 202, 1300–1303.
18 Henkart, M.P. (1975) Biophys. J. 15, 267a.

19 DiPolo, R., Requena, J., Brinley, F.J., Jr., Mullins, L.J. Scarpa, A. and Tiffert, T. (1976) J. Gen. Physiol. 67, 433–467.
20 Nathaniel, E.J.H. and Pease, D.C. (1963) J. Ultrastruct. Res. 9, 511–532.
21 Lasek, R.J. (1982) Phil. Trans. R. Soc. Lond. Ser. B, 299, 313–327.
22 De Weer, P. (1976) J. Gen. Physiol. 68, 159–178.
23 Conti, F., De Felice, L.J. and Wanke, E. (1975) J. Physiol. 248, 45–82.
24 Moore, L.E., Fishman, H.M. and Poussrt, D.J.M. (1979) J. Membr. Biol. 47, 99–112.
25 Llano, I., Webb, C.K. and Bezanilla, F. (1988) J. Gen. Physiol. 92, 179–196.
26 Fishman, H.M. and Tewari, K.P. (1990) Biophys. J. 57, 523a.
27 Gross, G.W., Lucas, J.H. and Higgins, L. (1983) J. Neurosci. 3, 1979–1993.
28 Metuzals, J. and Tasaki, I. (1978) J. Cell Biol. 78, 597–621.
29 Terakawa, S. and Nakayama, T. (1985) J. Membr. Biol. 85, 65–77.
30 Pant, H.C., Terakawa, S. and Gainer, H. (1979) J. Neurochem. 32, 99–102.
31 Lasek, R.J., Krishnan, N. and Kaiserman-Abramof, I.R. (1979) J. Cell Biol. 82, 336–346.
32 Schlaepfer, W.W. and Micko, S. (1978) J. Cell Biol. 78, 369–378.
33 Geiger, B. (1983) Biochim. Biophys. Acta 737, 305–341.
34 Drust, D.S. and Creutz, C.E. (1988) Nature 331, 88–91.
35 Meiri, H., Spira, M.E. and Parnas, I. (1981) Science 211, 709–712.
36 Anglister, L., Farber, I.C., Shahar, A. and Grinvald, A. (1982) Dev. Biol. 94, 351–365.
37 Cohan, C.S., Conner, J.A. and Kater, S.B. (1987) J. Neurosci. 7, 3588–3599.
38 Lipscombe, D., Madison, D.V., Poenie, M., Reuter, H., Tsien, R.Y. and Tsien, R.W. (1988) Proc. Natl. Acad. Sci. USA 85, 2398–2402.
39 Nishiye, H. (1977) Jap. J. Physiol. 27, 451–466.
40 De Mello, W.C. (1973) Proc. Natl. Acad. Sci. USA 70, 982–984.
41 Dyrks, T., Weidmann, A., Malthaup, G., Salbaum, J.M., Lemaire, H.-G., Kang, J., Muller-Hill, B., Masters, C.L. and Beyreuther, K. (1988) EMBO J. 7, 944–957.
42 Hirano, A. (1980) Acta Neuropathol. 50, 187–192.
43 Mitsumoto, H. and Bradley, W.G. (1985) in The Pathology of the Myelinated Axon (Adachi, M., Hirano, A. and Aronson, S.M., eds.), p. 126, Igaku-Shoin, New York.
44 Kamiya, N. and Kuroda, K. (1957) Proc. Jap. Acad. 33, 149–152.
45 Scott, R.E., Perkins, R.G., Zschunke, M.A., Hoerl, B.J. and Maercklein, P.B. (1979) J. Cell Sci. 35, 229–243.
46 Tank, D.W., Wu, E.-S. and Webb, W.W. (1982) J. Cell Biol. 92, 207–212.
47 Lemasters, J.J., Ji, S. and Thurman, R.G. (1981) Science 213, 661–663.
48 Standen, N.B., Stanfield, P.R., Ward, T.A. and Wilson, S.W. (1984) Proc. Roy. Soc. B 221, 455–464.
49 Stein, P. and Palade, P. (1988) Biophys. J. 54, 357–363.